

Energy Harvesting from Aeroelastic Flutter

*Soon-Duck Kwon¹⁾, Kyungmin Kim²⁾ and Seungho Lee³⁾

^{1), 2), 3)} *KOCED Wind Tunnel Center, Department of Civil Engineering,
Chonbuk National University, Chonju, Chonbuk, Korea*

¹⁾ sdkwon@chonbuk.ac.kr

ABSTRACT

This paper presents experimental and analytical results on an energy harvesting devices for powering the small electronic apparatuses in field applications. The devices utilize the T-shaped cantilever which hastens occurrence of aeroelastic flutter at a low wind speed. Two prototype devices respectively equipped piezoelectric and electromagnetic energy converters were designed and fabricated. In the piezoelectric energy converter, the piezoceramic patches glued at cantilever converts strain energy into electric energy. The relative motion of magnets induced by cantilever fluttering results electric generation at coils in the electromagnetic energy converter. Wind tunnel tests reveal that the devices can generate output power from a wind speed of 4 m/s, and can respectively provide maximum average power of 1.5 mW for piezoelectric converter and 1.2 mW for electromagnetic converter at wind speed of 10 m/s. In conclusion, this paper demonstrates a methodology for harvesting the power from freely available wind.

1. INTRODUCTION

Wireless sensors for structural health monitoring are widely used in order to keep civil structures safe. These wireless sensors are free from wires to send or receive a signal but still need batteries for electric power supply which results in periodic maintenance to change battery. Maintenance costs for battery use in wireless sensor applications are estimated at \$80-\$500 per replacement including labor which exceeds the sensor's cost (EERE 2008). Therefore it has been a strong demand for developing small energy harvesting devices for electronic apparatuses in various civil applications.

Small devices have been developed to convert the mechanical or natural energy into electricity for powering remotely located wireless sensors at civil structures. Structural vibrations and natural wind are good source for generating electricity. Vibration-based energy harvesters have been investigated by several researchers, however, these are not successfully applicable to civil structures because of low energy density. The vibration frequency of bridges is less than 10 Hz mostly and even less

¹⁾ Professor

²⁾ Graduate Student

³⁾ Senior Researcher

than 1 Hz at cable-supported bridges. Moreover peak acceleration of bridges is generally less than 1 m/s^2 . Structural vibrations of bridges are not sufficient for power generation. Anton and Sodano (2007), Mitcheson et al (2008), Priya and Inman (2009), Kamiński and Beeby (2010) provide intensive review for energy harvesting.

Natural wind is another source to obtain energy at civil structures. However, very limited research has been performed in the field of wind energy harvesting. Flowing wind has an advantage of a continuous source of energy. Miniaturization of traditional wind energy converter tends to lower their efficiency because of mechanical losses at bearings, and the relatively high viscous drag on the blades at low Reynolds numbers may deteriorate performance of the device. Therefore a new device is demanded for wind energy harvesting.

Taylor et al (2001) proposed a so-called 'energy harvesting eel' made up of a long strip of piezoelectric polymer bimorph material for harvesting energy from ocean or river-water flows. Isogai et al. (2003) proposed flapping airfoil section supported on spring and electromagnetic generator. Priya (2005) studied small scale windmill consisting of twelve piezoelectric bimorphs arranged in a circular array oscillated by a rotating fan. Zhu et al (2009) investigated a flapping of flag-like piezoelectric films similar to 'energy harvesting eel'. Tang et al. (2009) numerically studied the cantilevered flat plate in axial flow for energy transfer. Erturk et al. (2010) used the clamped beams with piezoceramic patches supporting an airfoil section. Zhu et al. (2010) investigated cantilever-based electromagnetic wind generator operating at 2.5 m/s with corresponding electrical output power of 0.47 mW . Other small scale piezoelectric fluid energy harvesters includes a flapping leaf attached at the PVDF stalk (Li and Lipson, 2009), a piezoelectric bimorph cantilever excited by Karman vortex (Pobering et al, 2010).

In this paper, energy harvesting devices have been studied to generate electricity from natural wind flow focusing on lowering flutter speed and minimizing device size. Configuration of the generic device was developed from wind tunnel tests. A T-shaped cantilevers respectively equipped piezoelectric converter and electromagnetic converter were fabricated and tested under the wind flow to determine the relationship among wind speed, generated power and electric load resistance. This paper presents experimental setup and results to develop the novel wind energy harvester.

2. FLUTTER INSTABILITY AND DEVICE CONFIGURATION

A series of wind tunnel tests were performed at the KOCED Wind Tunnel Center in Chonbuk National University in order to find generic configuration of energy harvesting device that would be easily fluttering at low wind speed. Basic shape of the present energy harvesting device was initiated from the H-shaped cross section of the Tacoma Narrow Bridge which collapsed due to aeroelastic flutter instability.

It was found from the preliminary wind tunnel tests that the shape and size of the leeward edge did not significantly affect the flutter onset speed. Consequently, the shape of the present energy harvesting device was developed to fit the T-shaped cantilever as shown in Fig. 1 (Kwon, 2010). As shown in the figure, this device consists of cantilever structure with tip plate. When wind blows from cantilever tip to its support, the cantilever starts to vibrate and its amplitude becomes significant due to flutter

phenomenon. The structure of this device consists of only a cantilever without requiring structural components. The T-shaped cantilever does not produce electric power in present form, and can be used for providing necessary vibration to energy converter.

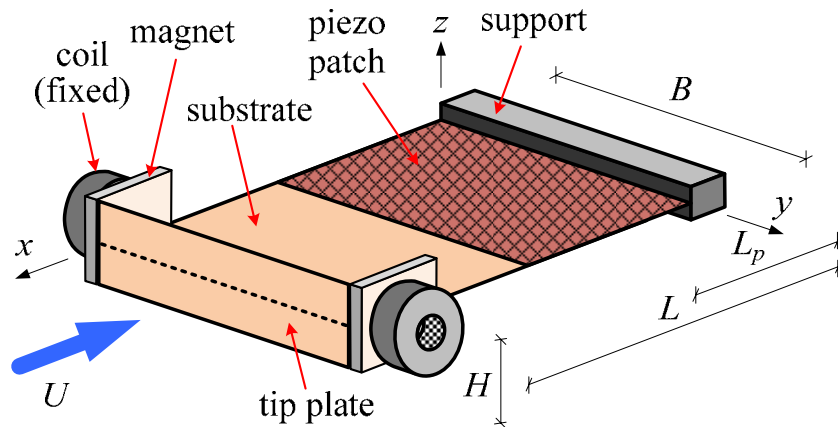


Figure 1. Configuration of present device for flutter energy harvesting.

Fig. 2 shows the measured tip displacement of the bare cantilever as a function of aspect ratio and wind speed. The tip displacements were normalized by its cantilever length. As shown in figure, the aspect ratio between cantilever length to tip height did not significantly affect flutter onset velocity and amplitude. However the flutter onset speed and cantilever tip displacement were sensitive to structural damping ratio. The following empirical relation between flutter onset velocity, fundamental frequency (f) and damping ratio (ξ) can be obtained from the measured responses.

$$U_f = (70\xi + 3)fL \tag{1}$$

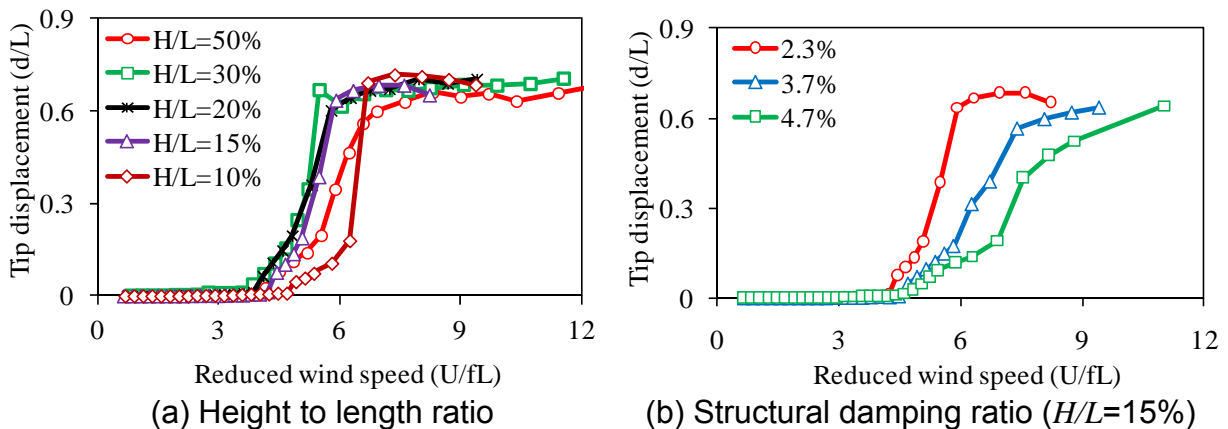


Figure 2. Normalized tip displacement of bare cantilever without energy converter.

Two kinds of system can be applied to the present cantilever for converting the wind-induced vibration into electric power. The first one is piezoelectric energy converter. The piezoceramic patches glued at both sides of cantilever also vibrate with substrate cantilever structure, and then the piezoelectric materials convert the strain energy into the electric energy. Details for the T-shaped cantilever with piezoceramic

patches are given in Section 3. The second one is electromagnetic energy converter. Oscillating magnets attached at cantilever and associated coils, or in reverse, can convert the vibration energy to electric energy. Details are explained at Section 4. Combination of these two energy converters is also applicable in the cantilever.

Total damping of the cantilever including energy converter consists of inherent structural damping, aerodynamic damping and electrical damping. In the wind speed below the flutter onset speed, all three damping dissipate the energy from the device. The inherent structural damping is constant at linear system, yet aerodynamic damping and electrical damping can be changed or adjusted according to wind speed and manipulation. When wind speed exceeds the threshold, flutter speed, aerodynamic damping becomes negative and pour energy from wind into the device inversely, and then the available harvesting energy gradually increases according to wind speed. As shown in Eq. (1), however, high electrical damping prevents occurrence of flutter at low wind speed and no energy can be harvested. Consequently proper control of electrical damping using electric load resistance is inevitable in the design of present device, and the results are given at next sections.

3. PIEZOELECTRIC ENERGY HARVESTING

3.1 Theory

The model for a cantilever beam with piezoelectric materials can be obtained with an energy method approach. The relationship between the current rate, current and velocity in piezoelectric material can be written as the following first order differential equation (duToit et al, 2005):

$$\theta \dot{d} + C_p \dot{v} + R^{-1}v = 0 \quad (2)$$

where ($\dot{}$) = time derivative; $d(=\phi r)$ = displacement; ϕ = mode shape; r = generalized coordinate; v = output voltage; R = electrical load resistance; C_p = capacitance; and θ = electro-mechanical coupling coefficient. If the vibration motion of the system is dominated by a specific mode, for example flutter phenomenon, the governing equation can be reduced to a scalar form:

$$\begin{Bmatrix} \dot{r}(t) \\ \ddot{r}(t) \\ \dot{v}(t) \end{Bmatrix} = \begin{bmatrix} 0 & 1 & 0 \\ -K/M & -C/M & \theta/M \\ 0 & -\theta/C_p & -1/RC_p \end{bmatrix} \begin{Bmatrix} r(t) \\ \dot{r}(t) \\ v(t) \end{Bmatrix} + \begin{Bmatrix} 0 \\ F(t)/M \\ 0 \end{Bmatrix} \quad (3)$$

where M = modal mass; C = modal damping; K = modal stiffness; ω = natural frequency ($=2\pi f$); and F = modal external force. After manipulating the above equations, the output voltage can be calculated from the tip displacement (d) of the harmonically excited cantilever as follows.

$$|v| = \frac{\theta}{\sqrt{C_p^2 + 1/(\omega R)^2}} |d| \quad (4)$$

The output power (P) can be obtained from the output voltage and applied external electrical resistance using the following relation.

$$P = v^2/R \quad (5)$$

The output power reaches maximum at an optimum external electrical resistance which is given as follows.

$$R^{opt} \approx \frac{1}{C_p \omega} \quad (6)$$

3.2 Prototype and Experimental Setup

Fig. 3 shows the experimental setup in the wind tunnel in order to investigate the aeroelastic response of the device (Kwon, 2010). The dimensions of the present cantilever were $L=100\text{mm}$, $B=60\text{mm}$, and $H=30\text{mm}$. The thickness of the aluminum substrate was 0.2 mm . The tip mass was 15.5g . The open circuit natural frequency at the first mode was 6.17 Hz and the inherent damping ratio including open circuit piezoceramics patches was 1.8% .

A total of six flexible PZT-5A piezoceramics (M-2814-P2 from Smart Material Corporation) were attached to the roots of both sides of the cantilever. The length and the width of each piezoceramic were 28 mm and 14 mm , respectively. As shown in Figure 3, three piezoceramics were attached side by side at 60mm wide substrate and the other three's were bonded at opposite surface symmetrically. 30mm from cantilever base was covered by piezoceramics and remaining 70mm to cantilever tip was consisted of aluminum substrate only. Piezoceramics were covered 19.6% of cantilever area. The electrodes of the piezoceramics were combined in series connection.

During the wind tunnel test, wind speed was measured using a pitot tube and pressure transducer (Setra 239). The images with speed of $120\text{ frames per second}$ were acquired at the CCD camera, and then time history of tip displacements were obtained from the image processing technique. The output voltage was monitored on the Agilent 34410A digital multimeter.

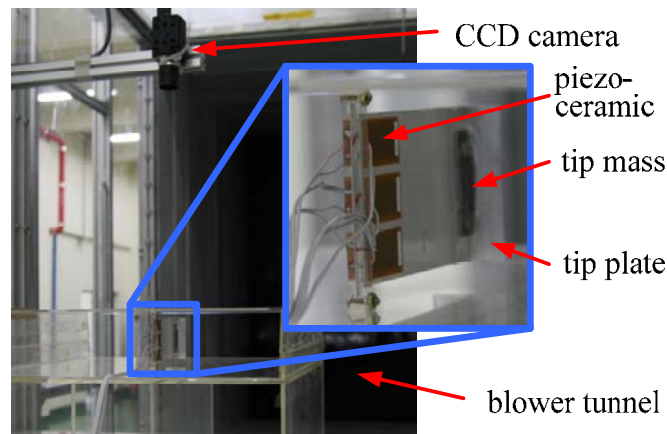


Figure 3. Prototype device with piezoceramic patches at wind tunnel.

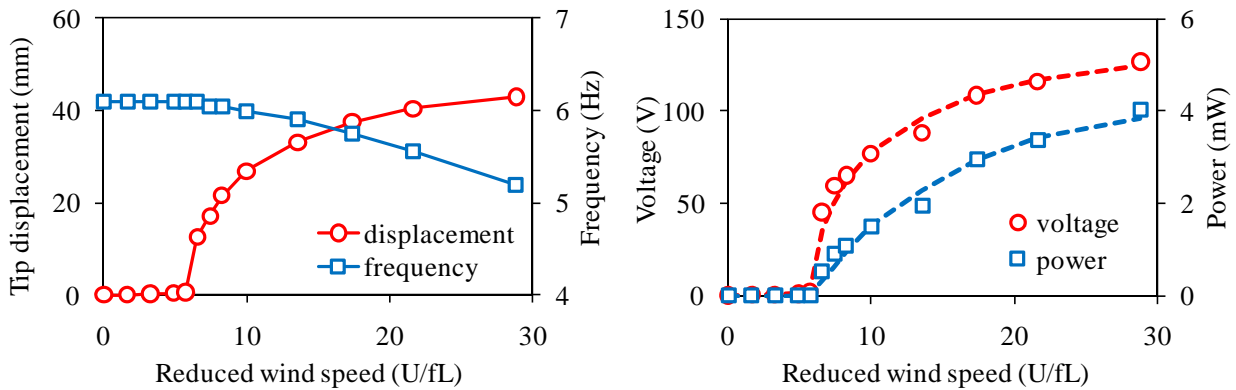
3.3 Test and analysis results

Fig. 4(a) shows the measured tip displacement of the cantilever with piezoceramics for $R=4\text{ M}\Omega$ according to wind speed. The cut-in wind speed corresponding to flutter onset speed was found to be 4.0 m/s . The cut-out wind speed, which is the maximum speed allowing for safe operation, was higher than 15 m/s . The tip displacement gradually increases according to wind speed after flutter onset, and converges to a

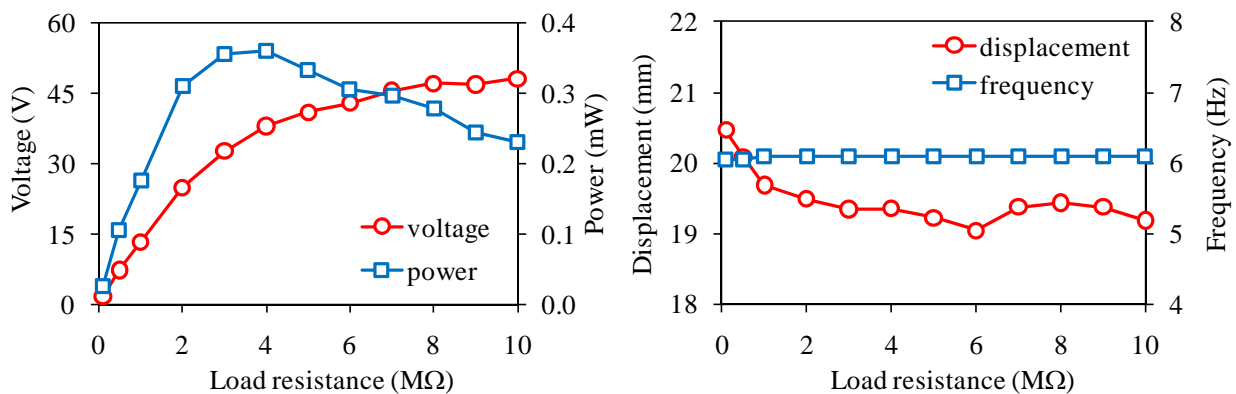
certain value without diverging because of the shunt damping effect of piezoelectric power generation.

As shown in Fig. 4(a), the vibration frequency was gradually reduced from 6.1 Hz with-out wind to 5.2 Hz at 15 m/s due to fluid structure interaction. Figure 4(b) shows the output voltage as a function of wind speed. The output voltage can be calculated from the tip displacement of the cantilever from Eq. (4). The magnitude of the measured output voltage was found to be consistent with the computed value. The maximum output power for an external electrical resistance of 4 MΩ was 4.0 mW.

Fig. 5(a) shows the output voltage and power at wind speed of 4.6 m/s versus electrical load resistance. The effect of load resistance on tip displacement and frequency is given in Fig. 5(b). Peak displacement decreased only 0.9 mm as the load resistance increased from 0.1 MΩ to 10 MΩ. The vibration frequencies given in Fig. 5(b) remained constant even after flutter occurrence. These results reveal that electrical load resistance does not significantly affect the mechanical behavior of cantilever at aeroelastic flutter.



(a) Tip displacement and vibration frequency (b) Output voltage and power
Figure 4. Tip displacement and output of the device (mark: measured, dotted line: calculated).



(a) Output voltage and power (b) Tip displacement and vibration frequency
Figure 5. Experimental responses at wind speed of 4.6 m/s as a function of external electrical resistance.

4. ELECTROMAGNETIC ENERGY HARVESTING

4.1 Theory

When the cantilever equipped magnets or coils is vibrated due to flutter, the governing equation describing relative movement of magnets with respect to coils, or in reverse, can be derived from equilibrium of the forces acting on a system. The axial component of electro-motive force opposing the motion along coil is simply given by:

$$F_{em} = \psi(z)i(t) \quad (7)$$

where i is the induced current in coil, and ψ is the electromagnetic coupling coefficient depending on magnetic field and coil length exposed to magnetic flux. The relationship between the current rate, current and relative velocity in coil can be written as the following first order differential equation in terms of resistance R , and the inductance of coil winding L_c (Kamierski and Beeby 2010, Beeby et al. 2007):

$$i(t) = \frac{\psi}{L_c} \dot{r}(t) - \frac{R}{L_c} i(t) \quad (8)$$

Substituting Eq. (7) into equation of motion for free vibration, and combining it with Eq. (8), the following equation of motion can be finally derived in state-space form:

$$\begin{Bmatrix} \dot{r}(t) \\ \ddot{r}(t) \\ \dot{i}(t) \end{Bmatrix} = \begin{bmatrix} 0 & 1 & 0 \\ -K/M & -C/M & -\psi/M \\ 0 & \psi/L_c & -R/L_c \end{bmatrix} \begin{Bmatrix} r(t) \\ \dot{r}(t) \\ i(t) \end{Bmatrix} + \begin{Bmatrix} 0 \\ F(t)/M \\ 0 \end{Bmatrix} \quad (9)$$

After manipulating the above equations, the output voltage can be calculated from the displacement of the harmonically excited cantilever as follows.

$$|v| = \frac{R\psi}{\sqrt{L_c^2 + (R/\omega)^2}} |d| \quad (10)$$

The output power can be obtained by applying the output voltage into the Eq. (5).

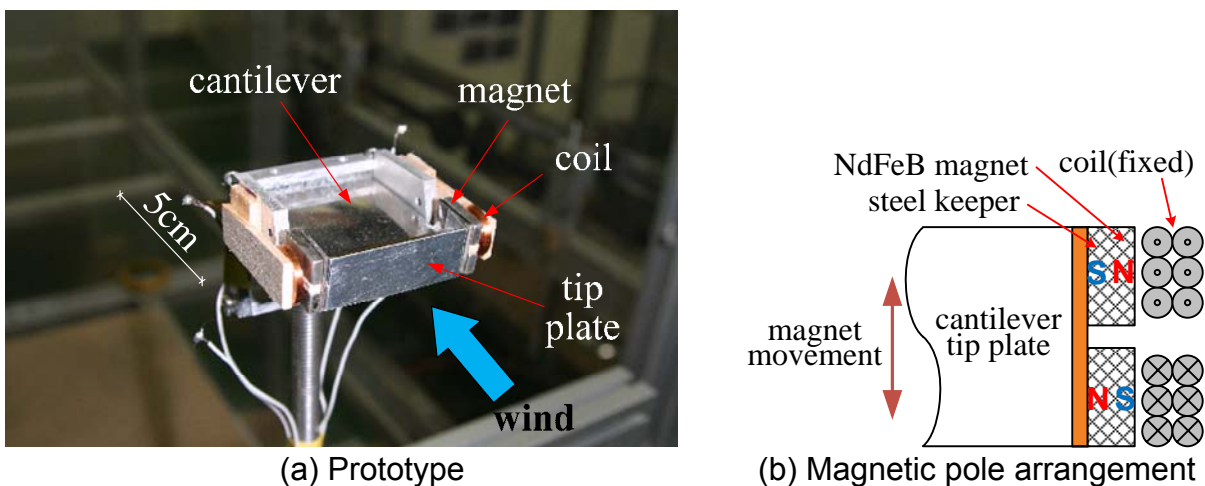


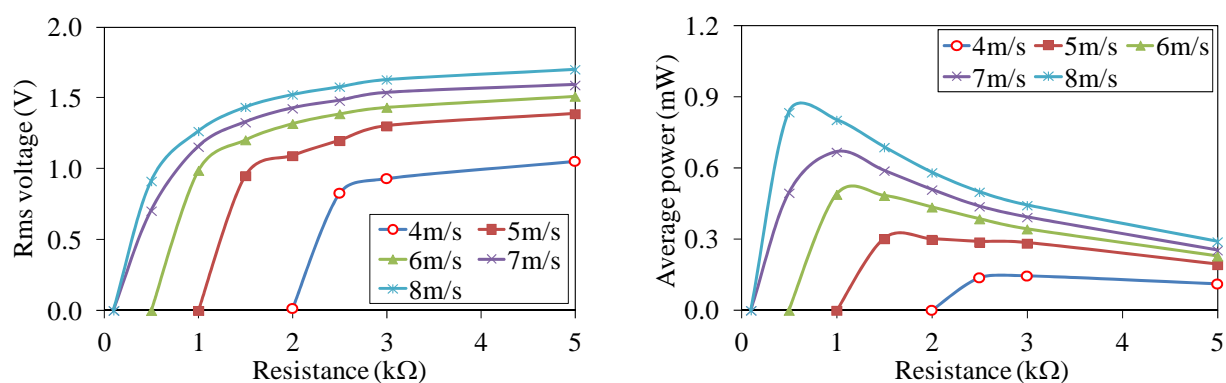
Fig. 6. Prototype device with electromagnetic converter at wind tunnel.

4.2 Prototype and Experimental Setup

Fig 6(a) shows the prototype device equipped electromagnetic converter and experimental setup in the wind tunnel. The dimensions of the present cantilever were $L=50\text{mm}$ (including support), $B=40\text{mm}$, and $H=15\text{mm}$. The cantilever was made of spring steel plate with thickness of 0.1 mm . The tip mass was 20g including tip plate, steel keeper and magnets. The open circuit natural frequency at the first mode was 5.67Hz , and corresponding inherent structural damping ratio was 0.4% .

The device uses two identical earth neodymium iron boron (NdFeB) magnets at each side of the cantilever tip. Size of a magnet was $15 \times 6.5 \times 3\text{ mm}^3$. The magnetic poles were aligned as shown in Fig 6(b) (Wang 2008). Two coils at each side of cantilever tip respectively have an outer diameter of 15mm , an inner diameter of 3mm and a thickness of 2mm . The coil consisted of 1200 turns of enamel coated copper wire with diameter of $90\text{ }\mu\text{m}$. Resistance and inductance of the coil were respectively $103\text{ }\Omega$ and 9.67 mH .

Cantilever displacement was measured from the Omron ZX-LD100L laser displacement transducer. The output voltage was monitored on the NI-PCI 6024E data acquisition board. The other measuring equipments were the same as those in previous section.



(a) Electric resistance vs rms voltage (b) Electric resistance vs average power
Fig. 7. Experimental results for relation among wind speed, electric resistance and electric output.

4.3 Test and analysis results

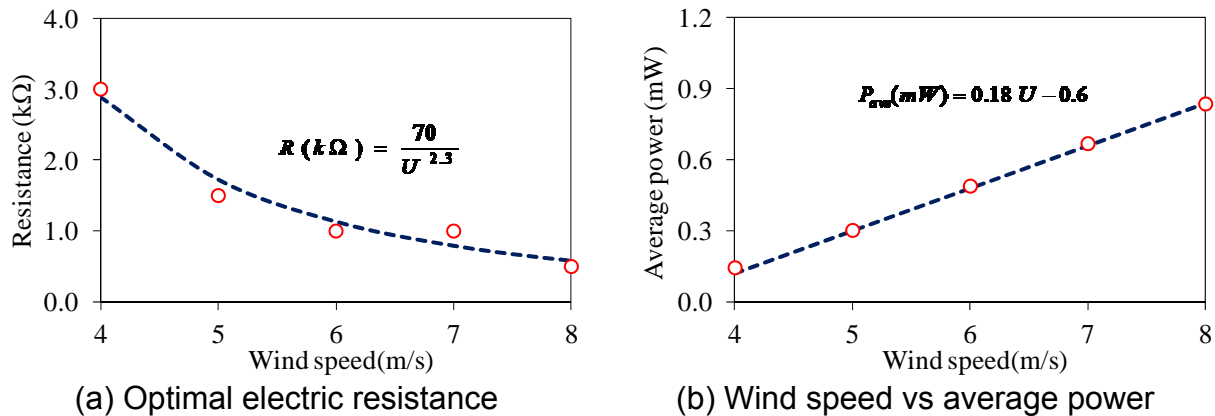
Fig. 7 shows the relation among wind speed, electric resistance and electric output obtained from wind tunnel tests. The output voltage gradually increases as electric load resistance increases, and converges to a certain value at open circuit. It is apparent from Fig. 7(b) that average harvested power from coils increases almost linearly with wind speed. On the other hand, the magnitude of matching electric load resistance drops down rapidly with increasing wind speeds. Optimal electric load where maximum power can be obtained is $3\text{ k}\Omega$ at 4 m/s but drops to $0.5\text{ k}\Omega$ at 8 m/s . However a little more drop of electric load from its optimal value prevents flutter occurrence and results zero power.

Fig. 8(a) summarizes the electric load resistance as a function of wind speed to get maximum average power. The power reaches maximum at an optimum electric load

which is empirically given as:

$$R^{opt} = \frac{70,000}{U^{2.3}} \quad (11)$$

Fig 8(b) reveals available power of the device as a function of wind speeds. Those results were obtained from wind tunnel tests when the optimal electric resistance shown in Fig 7(a) connected to coils. The average power linearly increases in proportion to the wind speed within the tested range. Fig 8(b) is power performance curve of the device with variable optima electric load resistance.



(a) Optimal electric resistance (b) Wind speed vs average power
 Fig. 8. Experimental results for optimal electric resistance and maximum available power as a function of wind speed.

5. CONCLUDING REMARKS

This study demonstrates an energy harvesting device from a freely available wind flow to provide electric power to wireless sensor network for structural health monitoring of various structures. The prototype devices activated by aeroelastic flutter equip piezoelectric and electromagnetic energy converters. The devices can generate output power from a wind speed of 4 m/s, and can respectively provide average power of 1.5 mW for piezoelectric converter and 1.2 mW for electromagnetic converter at wind speed of 10 m/s.

REFERENCES

- Anton, S.R. and Sodano, H.A. (2007), "A review of power harvesting using piezoelectric materials (2003–2006)", *Smart Materials and Structures*, 16.
- Beeby, S.P., et al. (2007), "A micro electromagnetic generator for vibration energy harvesting", *J. of Micromechanics and Microengineering* 17(7).
- duToit, N.E., Wardle, B.L. and Kim, S.K. (2005) "Design considerations for MEMS-scale piezoelectric mechanical vibration energy harvesters", *Integrated Ferroelectrics*, 71.
- EERE (2008), http://www1.eere.energy.gov/industry/sensors_automation/pdfs/kcf_vibrationpower.pdf.
- Erturk, W.G. Vieira, C. De Marqui, Jr., and D.J. Inman, (2010), "On the energy harvesting potential of piezoaeroelastic systems", *Applied Physics Letter*, 96, 184103.

- Isogai, K., Yamasaki, M., Matsubara, M. and Asaoka, T. (2003), "Design study of Elastically Supported Flapping Wing Power generator", International forum on Aeroelasticity and Structural Dynamics, Amsterdam, Netherland.
- Kamierski, T.J. and Beeby, S. (Eds.) (2010), Energy Harvesting Systems: Principles, Modeling and Applications, Springer.
- Kwon, S.D. (2010), "A T-shaped piezoelectric cantilever for fluid energy harvesting", Applied Physics Letter, 97, 164102.
- Li, S. and Lipson, H. (2009), "Vertical-stalk flapping-leaf generator for wind energy harvesting", Proceedings of the SMASIS, Oxnard, USA.
- Mitcheson, P.D., et al. (2008), "Energy harvesting from human and machine motion for wireless electronic devices", *Proceedings of the IEEE*, 96(9).
- Pobering, S., Ebermyer, S. and Schwesinger, N. (2010), "Energy harvesting under induced best conditions", Proceedings of IMAC-XXVIII, Jacksonville, USA.
- Priya, S. (2005), "Modeling of electric energy harvesting using piezoelectric windmill", Applied Physics Letter, 87, 184101.
- Priya, S. and Inman, D. J. (Eds.) (2009), Energy Harvesting Technologies, Springer. Smart Material Corporation, <http://www.smart-material.com/>.
- Tang, L., Paidoussis, M.P. and Jiang, J. (2009), "Cantilevered flexible plates in axial flow: Energy transfer and the concept to flutter-mill", J. of Sound and Vibration, 326.
- Taylor, G.W., et al. (2001), "The energy harvesting eel: A small subsurface ocean/river power generator", IEEE J. of Oceanic Engineering, 26.
- Wang, L., et al. (2008), "Integrated approach to energy harvester mixed technology modeling and performance optimization", Design, Automation and Test in Europe, DATE '08, Munich, Germany.
- Zhu, D., et al. (2010), "A novel miniature wind generator for wireless sensing applications", Sensors, 2010 IEEE, Hawaii, USA.
- Zhu, Q., Haase, M., and Wu, C.H. (2009), "Mode coupling and flow energy harvesting by a flapping foil", Physics of Fluids, 21, 033601.